Statistical properties and broken symmetries within the shell model

J. F. Shriner, Jr.*
Department of Physics, Tennessee Technological University, Cookeville, Tennessee 38505

G. E. Mitchell†
Department of Physics, North Carolina State University, Raleigh, North Carolina 27695 and Triangle Universities Nuclear Laboratory, Durham, North Carolina 27708

B. A. Brown‡
Department of Physics and Astronomy and National Superconducting Cyclotron Laboratory, Michigan State University, East Lansing, Michigan 48824-1321

(Received 5 August 2004; published 25 February 2005)

Shell-model calculations in the *s-d* shell have been utilized to examine how the statistical behavior of eigenvalues and reduced transition probabilities are affected by broken isospin symmetry. Calculations have been performed for the nuclides ^{22}Na, ^{26}Al, and ^{34}Cl and have been compared to existing experimental data for ^{26}Al and ^{30}P. The eigenvalue statistics depend on the magnitude of the Coulomb matrix element, and this is reflected in a sensitivity to the choice of single-particle energies. The distributions of reduced transition probabilities are not universal but depend upon the particular transition mode chosen; this behavior is qualitatively similar to experimental results.

DOI: 10.1103/PhysRevC.71.024313 PACS number(s): 24.80.+y, 21.60.Cs, 24.60.Ky

I. INTRODUCTION

Random-matrix theory (RMT) has been used to describe certain statistical properties of nuclear levels since the early work of Wigner [1] almost 50 years ago. Significant developments in the early years included discussion of reduced width distributions by Porter and Thomas [2], the extension to reduced width amplitude distributions by Krieger and Porter [3], and the exploration of eigenvalue statistics in a series of papers by Dyson and Mehta [4–9]. A monograph summarizing the status of RMT at the time was published by Mehta in 1967 [10].

Ensuing years provided not only the additional development of the theory but also the acquisition of high quality data that provided some of the first good experimental tests of random-matrix theory. The Gaussian orthogonal ensemble (GOE) version of RMT was utilized to describe statistical properties of neutron resonances by the Columbia group (e.g., [11,12]) and proton resonances by the TUNL group (e.g., [13,14]). The status of RMT in the early 1980s was summarized in a review by Brody *et al*. [15].

Interest in RMT showed a resurgence after Bohigas, Giannoni, and Schmit suggested in 1984 a connection between RMT and chaos [16]. Analysis of numerous theoretical systems was consistent with this conjecture and suggested that RMT could be a valuable tool for studying chaos and regularity in quantum systems. A second, expanded edition of Mehta's monograph was published [17]. Although it had long been realized that RMT should apply to systems other than just nuclear ones (see, e.g., [18]), interest in applying random-matrix theory to non-nuclear systems expanded greatly once a connection with chaos was established. A new, comprehensive review of random-matrix theory was published by Guhr, Müller-Groeling, and Weidenmüller in 1998 [19].

Comparison of RMT with experimental data requires knowledge of the symmetries of the system, since the predictions of RMT in their simplest forms apply only to a set of levels which share the same symmetries. This aspect of random-matrix theory is one of the primary reasons why there are relatively few experimental tests of RMT. This is especially true in nuclear physics. Such tests require data of exceptional quality: the set of levels must be both complete (few or no missing levels) and pure (few or no spurious levels due to mistakenly identifying a level or to incorrect quantum number assignments to a true level). Failure to meet this requirement biases the data so strongly that eigenvalue statistics for such data convey little if any information (the situation is not as severe for transition statistics).

Despite these difficulties, in recent years there has been significant progress, both theoretical and experimental, in moving beyond systems where all quantum numbers are good to understand how broken symmetries affect eigenvalue and transition statistics. In this paper, we utilize the nuclear shell model to examine how both eigenvalue and transition statistics are affected by breaking of isospin symmetry in the *s-d* shell. We review in Sec. II some of the previous work dealing with broken symmetries, and we present details of the specific shell-model calculations analyzed here. Section III discusses the statistics used and methods of analysis. Eigenvalue statistics of shell-model calculations for the nuclides ^{22}Na, ^{26}Al, and ^{34}Cl are discussed in Sec. IV (the work on ^{26}Al has already been published [20]), and transition statistics for those same nuclides are presented in Sec. V. The results are summarized in Sec. VI.

*Email address: jshriner@tntech.edu.
†Email address: mitchell@tunl.duke.edu.
‡Email address: brown@nscl.msu.edu.

II. BACKGROUND

A. Broken symmetries

General discussion of how a broken symmetry would affect eigenvalue statistics dates back to Dyson in 1962 [7], and it was again discussed in detail by Pandey in 1981 [21]. Their findings can be summarized by Pandey's statement that "even a small breaking of a fundamental or model symmetry is shown to yield fluctuation patterns which would be found in the complete absence of the symmetry."

The first experimental data suitable for testing these ideas were from ^{26}Al. Careful study of the ^{25}Mg(p,γ) reaction by Endt and collaborators [22,23] had been combined with previous measurements on the ^{26}Al system to establish a detailed level scheme; comparison with shell-model calculations [24] suggested that the positive-parity levels were pure and complete from the ground state up to $E_x \approx 8$ MeV. This provided the first time in a nuclear system that data were considered pure and complete over such a large energy range. Analysis of eigenvalue statistics [25,26] showed behavior that was attributed to isospin symmetry breaking. A subsequent theoretical study by Guhr and Weidenmüller [27] demonstrated that this interpretation was consistent with the ^{26}Al data. Hussein and Pato [28] obtained similar results. Subsequently, measurements were performed to establish a complete level scheme in a second nuclide, ^{30}P [29], and these data showed very similar behavior for the eigenvalue statistics [30].

Additional experiments in "analog" systems—classical systems that mimic quantum systems in that they have energy eigenvalues—have allowed experimentalists to study how the eigenvalue statistics change as the amount of symmetry breaking is varied. High-statistics measurements of acoustic resonances in quartz blocks [31] and of microwave resonances in superconducting cavities [32] are consistent with RMT predictions.

Transition statistics have also played an important role in our understanding of statistical properties. For example, width distributions have been utilized for many years to estimate the number of missing levels in the determination of level densities near the neutron separation energy. In this area, however, the understanding of how a broken symmetry affects the statistics has trailed that of eigenvalue statistics. When a system's symmetries are all good ones, its reduced widths are expected to follow a Porter-Thomas distribution [2]—a χ^2 distribution with one degree of freedom. However, the distribution of reduced transition probabilities in ^{26}Al appears to show a deviation from the Porter-Thomas distribution [33]. While the distribution is certainly distorted somewhat by the fact that the smallest transitions are not observed experimentally, this effect did not appear to explain the deviation. Again the suggestion was that this deviation was a consequence of the broken isospin symmetry. At the time there was no theoretical guidance as to how this distribution was affected by a broken symmetry. Soon thereafter, two independent studies by Barbosa, Guhr, and Harney [34] and by Hussein and Pato [35] showed that symmetry breaking could affect the reduced transition probability distributions in a manner at least qualitatively consistent with the ^{26}Al data. A second set of experimental data for ^{30}P also showed similar behavior [30]. A recent analog measurement of two coupled superconducting microwave cavities determined the distribution of the product of partial widths [36], and it was found that the experimental data deviate from the K_0 distribution (the product of two Porter-Thomas distributions).

B. Shell model

To explore the question of how a broken symmetry affects transition strength distributions in a manner that avoids completely the issue of missing transitions, we have utilized the nuclear shell-model code OXBASH [37] to perform calculations for the *s-d* shell nuclides ^{22}Na, ^{26}Al, and ^{34}Cl. Nuclides in the *s-d* shell were chosen because the available experimental data, for ^{26}Al and ^{30}P, are in that mass region. Calculations were performed both for an isospin-conserving (IC) Hamiltonian and for a Hamiltonian which did not conserve isospin (hereafter labeled INC); the INC calculations utilized the method of Ormand and Brown [38]. For ^{26}Al, two different sets of single-particle energies were utilized with the INC Hamiltonian—one set based on the $A = 39$ system, labeled INC$_A$, and the other based on the $A = 17$ system, labeled INC$_B$.

The calculation is carried out in the proton-neutron formalism with the two-body interaction from Ref. [38]. The two-body part of the interaction is obtained with the USD Hamiltonian for the isospin-conserving part plus (a) the Coulomb interaction between two protons, (b) a charge-dependent strong interaction between protons and neutrons, and (c) a small charge-symmetry breaking interaction. The single-particle part of the Hamiltonian was taken either from the spectra of ^{39}Ca-^{39}K (INC$_A$) or from the spectra of ^{17}F-^{17}O (INC$_B$). The 400 keV shift of the $s_{1/2}$ state in ^{17}F relative to ^{17}O is understood as a Thomas-Ehrman shift of the loosely bound $s_{1/2}$ single-particle state outside of an ^{16}O closed shell. The calculation of the Thomas-Ehrman shift requires the use of a Woods-Saxon potential (with the Coulomb interaction for protons) with the neutron single-particle energy constrained to the experimental value in ^{17}O. Our application of a constant Thomas-Ehrman shift to all of the many-body states is an approximation. A better calculation would require an expansion of the n-particle wave functions in terms of the parentage to the complete set of $(n-1)$-particle wave functions with an analysis of the associated spectroscopic factors and separation energies for the $1s_{1/2}$ orbit. This is beyond the scope of the present paper, but it should be considered in future analyses.

An analysis of level statistics for ^{26}Al has already been published [20] and suggests that experimental data are better described by INC$_B$.

Because we were interested in comparisons with experimental data for ^{26}Al and ^{30}P, our analysis has focused on states with spins in the range $0-5$. The lowest 30 positive-parity eigenvalues for each spin were determined; the energies of the 30th eigenvalues for each spin set were compared, and the one with the lowest energy was identified. All energy eigenvalues with energies less than or equal to this state were then considered for further analysis; this ensured that we had a

TABLE I. Summary of shell-model calculations in ^{22}Na, ^{26}Al, and ^{34}Cl.

Nuclide	S_p (Exp.) (MeV)	Hamiltonian[a]	E_{max} (MeV)	Number of levels
^{22}Na	6.739	IC	11.279	121
		INC$_A$	11.222	121
^{26}Al	6.307	IC	9.107	132
		INC$_A$	9.056	132
		INC$_B$	8.961	133
^{34}Cl	5.143	IC	10.076	123
		INC$_A$	10.123	123

[a]INC$_A$ refers to $A = 39$ single-particle energies; INC$_B$ refers to $A = 17$ single-particle energies.

complete set of positive-parity eigenvalues for the spin range in question. Information about each calculation is summarized in Table I.

In this energy range for these particular nuclides, all states in the IC calculations have isospin values of either $T = 0$ or $T = 1$. In the INC calculations, each state's wave function contains a mixture of $T = 0$ and $T = 1$ components. The isospin mixing comes from the j dependence of the isovector single-particle energies and the J dependence of the isovector and isotensor two-body matrix elements. If these isovector and isotensor matrix elements are constant (all the same for each kind) there is a constant Coulomb displacement energy and no isospin mixing. The INC interaction is based upon the Coulomb contribution calculated in an oscillator basis plus an INC strong interaction with strengths obtained from the experimental Coulomb displacement energies. For INC$_A$, the isospin mixing is dominated by the J dependence of the two-body INC matrix elements. However, the j dependence of the single-particle energies in INC$_B$ is much larger than that of INC$_A$ due to the 400 keV Thomas-Ehrman shift of the $s_{1/2}$ orbit in $A = 17$ relative to the $d_{5/2}$ orbit. This results in isospin mixing matrix elements for ^{26}Al which are about four times larger with INC$_B$ compared to INC$_A$.

For the INC calculations, states are classified according to their dominant isospin. The dominant isospin is determined by calculating the overlaps of each INC wave function with the IC wave functions for the same spin. The state is then assigned $T = 0$ or $T = 1$ according to which isospin component is larger. The majority of states remain dominated by a single isospin; this is not surprising since the average level spacings at the highest energies for states of a single J are $\approx$20 times the rms interaction matrix element for INC$_A$ and $\approx$4 times the rms matrix element for INC$_B$.

Reduced transition probabilities were calculated for each possible $M1$ and $E2$ transition among the complete set of states. The transition operators were the same in the IC and INC calculations; in the INC case, the isospin mixing occurs because of mixing in the wave functions. Unlike the case of experimental data, the calculations determine $B(M1)$ and $B(E2)$ for even the weakest transitions and therefore provide a very large and complete data set. For the IC calculations, each transition is identified as isoscalar (IS) if the initial and final states have the same isospin and as isovector (IV) if the initial and final states have different isospins. For the INC calculations, the identification of a transition as isoscalar or isovector is based on the dominant isospins (as defined above) of the initial and final states. A summary of the number of transitions and the average $B(M1)$ and $B(E2)$ values are given in Table II.

III. ANALYSIS METHODS

In this section, we summarize the methods of analysis applied to these calculations.

A. Eigenvalues

As discussed above, the simplest eigenvalue statistics of random-matrix theory apply to a group of levels which share the same symmetries. In nuclear physics, applicable symmetries are generally the total angular momentum J and parity π; other quantum numbers such as isospin T or the K quantum number may also be relevant in some situations. In the s-d shell at low energies, T is a useful quantum number even though it is slightly broken. Therefore, we classify the states according to their values of J^π and T.

We utilize the term *sequence* to mean a subset of the levels which share one or more quantum numbers; a pure sequence will be a sequence in which the levels have all of their quantum numbers the same. Therefore, for these data, a pure sequence

TABLE II. Summary of shell-model transition calculations in ^{22}Na, ^{26}Al, and ^{34}Cl. N is the number of transitions in the sequence.

Nuclide	Hamiltonian	$M1_{IS}$		$M1_{IV}$		$E2_{IS}$		$E2_{IV}$	
		N	$B(M1)_{avg}$ (W.u.)	N	$B(M1)_{avg}$ (W.u.)	N	$B(E2)_{avg}$ (W.u.)	N	$B(E2)_{avg}$ (W.u.)
^{22}Na	IC	1971	0.00037	1794	0.18	2925	2.6	2532	0.11
^{22}Na	INC$_A$	1970	0.015	1793	0.16	2924	2.3	2531	0.41
^{26}Al	IC	2464	0.00027	1918	0.11	3653	2.9	2696	0.073
^{26}Al	INC$_A$	2464	0.0032	1919	0.11	3654	2.8	2697	0.19
^{26}Al	INC$_B$	2561	0.013	1900	0.096	3756	2.5	2708	0.53
^{34}Cl	IC	2023	0.00041	1919	0.072	2930	2.4	2654	0.13
^{34}Cl	INC$_A$	2023	0.0047	1919	0.068	2930	2.2	2654	0.28

consists of a group of levels that share the same J^π and T values. We compare the behavior of the pure sequences to that of mixed sequences identified by their J^π values only.

We utilize two common eigenvalue statistics, the nearest-neighbor spacing distribution (NNSD) first described by Wigner [1] and the Δ_3 statistic introduced by Dyson and Mehta [8]. The NNSD emphasizes short-range correlations, whereas Δ_3 reflects long-range correlations ("spectral rigidity") in the eigenvalue spectrum. For a pure sequence of eigenvalues, the GOE prediction for the NNSD is essentially the Wigner distribution,

$$P(x) = \frac{\pi x}{2} e^{-\pi x^2/4}, \tag{1}$$

where $x \equiv S/D$; S is a nearest-neighbor spacing, and D is the average spacing. On the other hand, a group of levels with infinitely many pure sequences included in it would show an NNSD that followed a Poisson distribution:

$$P(x) = e^{-x}. \tag{2}$$

An interpolation formula between these two extremes has been defined by Brody [39] as

$$P(x;\omega) = \alpha\,(\omega+1)\,x^\omega e^{-\alpha x^{\omega+1}}$$
$$\alpha = \left[\Gamma\left(\frac{\omega+2}{\omega+1}\right)\right]^{\omega+1}, \tag{3}$$

where $\omega = 1$ corresponds to the GOE distribution and $\omega = 0$ corresponds to the Poisson distribution. While no physical meaning has been attached to the parameter ω, it has become the common way of characterizing such distributions. When all quantum numbers represent conserved quantities, sets of eigenvalues which contain a finite number of pure sequences (but more than one) are expected to show NNSD's between the GOE and Poisson distributions; the exact distribution depends on the number of pure sequences and the relative sizes of those sequences.

In addition to the short-range correlations among the eigenvalues, the GOE also predicts long-range correlations. The Dyson-Mehta Δ_3 statistic is commonly used to study these long-range effects. This statistic is defined as

$$\Delta_3(L) = \min_{A,B} \frac{1}{E_{\max} - E_{\min}} \int_{E_{\min}}^{E_{\max}} [N(E) - AE - B]^2 dE. \tag{4}$$

Here, L is the number of average spacings in the energy interval $[E_{\min}, E_{\max}]$, and $N(E)$ is the number of levels with energies less than or equal to E. The Δ_3 statistic is a measure of the deviation of $N(E)$ from the best straight-line fit.

The long-range order predicted by random-matrix theory manifests itself in Δ_3 as a logarithmic behavior. For GOE statistics, the expected value for large L approaches

$$\Delta_{3_{\rm GOE}}(L) \approx \frac{1}{\pi^2}\left[\ln L - 0.0687\right]. \tag{5}$$

Poisson statistics, on the other hand, produce an expected value of $L/15$. Once again, an interpolation formula between GOE and Poisson behavior is available. Seligman and Verbaarschot [40] have shown semiclassically that if phase space is divided into a chaotic region with fraction μ of the phase space and integrable regions with total fraction $1-\mu$, then

$$\Delta_3(L) = \Delta_{3_{\rm GOE}}(\mu L) + \Delta_{3_{\rm Poisson}}([1-\mu]L). \tag{6}$$

The value $\mu = 1$ corresponds to a GOE description, while $\mu = 0$ corresponds to Poisson statistics. As was true with the NNSD, the effect of impure level sequences when all quantum numbers are good is to move the Δ_3 distribution toward the Poisson result.

In both cases, before comparing the eigenvalue statistics for a data set with the theoretical expectations, it is necessary to account for the fact that the average spacing decreases as a function of energy. The method we utilize to do that has been outlined in detail in Ref. [41].

We note that a previous study of these two statistics with the shell model was performed by Ormand and Broglia [42]. That work included isospin breaking and showed generally good agreement with the GOE predictions. However, it included levels at significantly higher energies than those in this paper and, therefore, represents behavior in a different range of energies than the current work.

B. Transitions

To study the transitions, we utilized the distributions of reduced transition probabilities. We define a *transition sequence* as a set of reduced transition probabilities which have the same electric or magnetic character, the same multipolarity, and the same isospin characterization (isoscalar or isovector). Thus, these calculations have four distinct transition sequences: $M1_{\rm IS}$, $M1_{\rm IV}$, $E2_{\rm IS}$, and $E2_{\rm IV}$. Each transition sequence is analyzed independently.

It has been traditional to express the distributions in terms of a dimensionless variable by normalizing the B values by their local average:

$$y = B/\langle B\rangle. \tag{7}$$

When all quantum numbers are good, the expectation is that a single transition sequence will show behavior that follows the Porter-Thomas distribution:

$$P(y) = (2\pi y)^{-1/2}\, e^{-y/2}. \tag{8}$$

However, there are two good reasons to change to a logarithmic variable $z = \log_{10} y$. One is that the values of y typically cover a wide range, and logarithmic variables are convenient in such situations. The other is that various model studies [43–46] have suggested that transition strengths in chaotic systems follow a $\chi^2(\nu)$ distribution with $\nu = 1$ (the Porter-Thomas distribution) whereas transition strengths in integrable systems follow a $\chi^2(\nu)$ distribution with $\nu < 1$. When expressed in terms of the variable z, the χ^2 probability density functions have a maximum at $z = 0$ for all values of ν; therefore, expressing results in terms of the variable z allows a simpler comparison with the entire family of χ^2 density functions. In terms of z, the Porter-Thomas probability density function is

$$P(z) = \ln 10\,(z/2\pi)^{1/2}\, e^{-z/2}. \tag{9}$$

TABLE III. Spacing distribution and Δ_3 fits in shell-model calculations, along with experimental values, for ^{26}Al and ^{30}P. For each set of levels, results are presented for the case when the data are sorted into sequences identified by J^π and T and for the case when the data are sorted into sequences identified only by J^π.

Nuclide	Hamiltonian	Sequence identifiers	$N_{spacings}$	ω	μ
^{22}Na	IC	$J^\pi;T$	105	1.31 ± 0.16	1.10 ± 0.02
		J^π	115	$0.34^{+0.10}_{-0.11}$	0.75 ± 0.02
	INC_A	$J^\pi;T$	105	1.32 ± 0.16	1.09 ± 0.02
		J^π	115	$0.37^{+0.10}_{-0.11}$	0.75 ± 0.02
^{26}Al	IC	$J^\pi;T$	112	0.89 ± 0.13	0.99 ± 0.02
		J^π	126	0.49 ± 0.10	0.81 ± 0.02
	INC_A	$J^\pi;T$	112	0.87 ± 0.13	0.98 ± 0.02
		J^π	126	0.46 ± 0.10	0.79 ± 0.02
	INC_B	$J^\pi;T$	113	0.77 ± 0.12	0.92 ± 0.03
		J^π	127	0.48 ± 0.10	0.80 ± 0.02
^{34}Cl	IC	$J^\pi;T$	108	1.07 ± 0.15	1.10 ± 0.02
		J^π	117	0.43 ± 0.11	0.84 ± 0.03
	INC_A	$J^\pi;T$	108	1.09 ± 0.15	1.10 ± 0.02
		J^π	117	0.54 ± 0.11	0.87 ± 0.02
^{26}Al	Exp.	$J^\pi;T$	118	0.51 ± 0.11	0.93 ± 0.04
		J^π	133	0.47 ± 0.10	0.85 ± 0.02
^{30}P	Exp.	$J^\pi;T$	64	0.47 ± 0.15	0.93 ± 0.04
		J^π	87	0.39 ± 0.12	0.84 ± 0.06

Following Barbosa *et al*. [34], we utilize a generalized entropy to compare the calculations with a theoretical model:

$$S = -\int p(x) \ln \frac{p(x)}{P(x)}\, dx, \tag{10}$$

where $p(x)$ is the probability density function of the calculations, and $P(x)$ is the probability density function of the model, in this case the Porter-Thomas distribution. This quantity will vanish if and only if $p = P$, and it will be negative otherwise. In practice, we histogram the calculations into bins with centroids x_k and widths Δx_k. The appropriate approximation is then

$$S \approx -\sum_k p(x_k) \ln \frac{p(x_k)}{P(x_k)}\, \Delta x_k. \tag{11}$$

In order to allow for changes in $\langle B \rangle$ with energy, we determine those values locally for each transition. For a transition from an initial state E_i to a final state E_f, the corresponding value of $\langle B \rangle$ is determined by averaging all reduced transition probabilities from the appropriate transition sequence that have their initial and final states within 10 states of the initial and final states of the transition in question.

IV. EIGENVALUE ANALYSES

As described in Sec. III, nearest-neighbor spacing distributions can be characterized by the parameter ω, and the Δ_3 statistic can be characterized by the parameter μ. Those values are listed in Table III for the various shell-model calculations as well as for experimental data in ^{26}Al and ^{30}P.

We show the results for nearest-neighbor spacing distributions for the three ^{26}Al calculations and the ^{26}Al experimental data in Fig. 1 and for the two ^{34}Cl calculations in Fig. 2. The

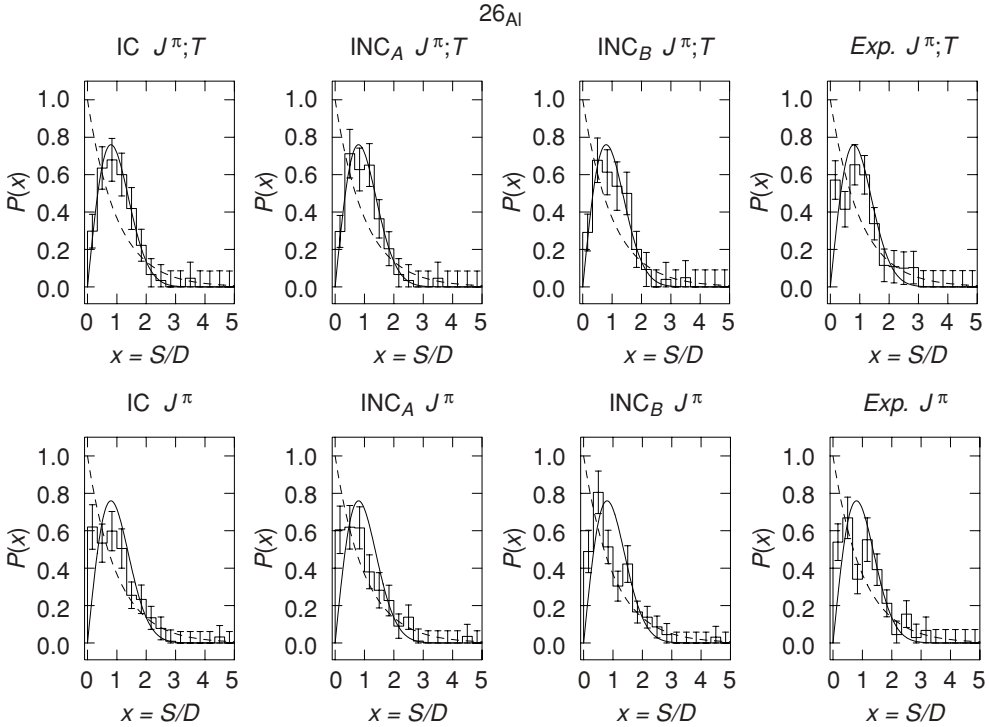

FIG. 1. Nearest-neighbor spacing distributions for shell-model eigenvalues and experimental eigenvalues in ^{26}Al. The labels on each graph indicate which quantum numbers identify the sequences and which Hamiltonian was used in the calculation. Solid curves show GOE distributions, and dashed curves show the corresponding Poisson distributions.

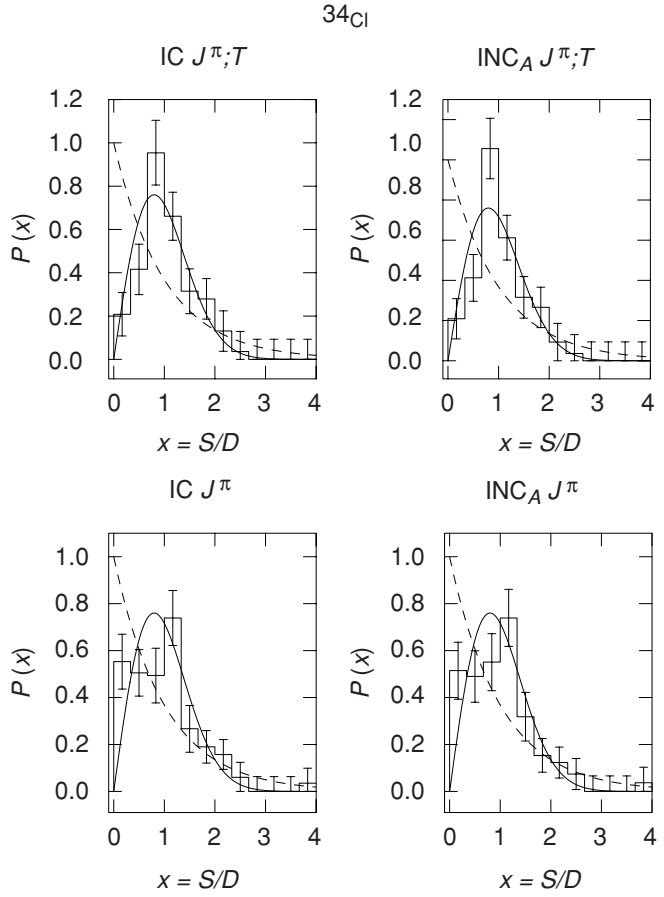

FIG. 2. Nearest-neighbor spacing distributions for shell-model eigenvalues in ^{34}Cl. The labels on each graph indicate which quantum numbers identify the sequences and which Hamiltonian was used in the calculation. Solid curves show GOE distributions, and dashed curves show the corresponding Poisson distributions.

results for Δ_3 are shown for ^{26}Al in Fig. 3 and for ^{22}Na in Fig. 4.

Several results are apparent. One is that while the ^{26}Al and ^{34}Cl IC results are in reasonable agreement with the GOE prediction, both ω and μ are larger than 1 for the ^{22}Na IC results; these calculations show even more level repulsion in this nuclide than is predicted by the GOE. It is not clear why this is so.

Another notable result is that as measured by these two eigenvalue statistics, there is little difference between the isospin-conserving calculations and the INC$_A$ calculations: the values of both ω and μ are essentially unchanged. This suggests that the amount of isospin mixing in this particular INC calculation is relatively small.

In contrast, the INC$_B$ calculations do show differences from the IC calculations. As explained in Sec. II, the Coulomb matrix element is significantly larger in INC$_B$ than in INC$_A$ ($\approx$24 keV in INC$_B$ for ^{26}Al as opposed to $\approx$6 keV in INC$_A$). This manifests itself as changes of ω from 0.89 ± 0.13 to 0.77 ± 0.12 and of μ from 0.99 ± 0.02 to 0.92 ± 0.03.

However, the INC$_B$ NNSD still shows significant differences from the experimental data in two ways. One is that the value of ω for the ^{26}Al experimental data is lower than it is for the calculation (0.51 ± 0.11 vs. 0.77 ± 0.12), although the large uncertainties make it difficult to draw a definitive conclusion. The second is that ignoring T as a quantum number makes no difference to the value of ω for the experimental data, whereas ignoring T causes a large drop in values of ω for the calculation. This large drop in ω is what would be expected if T were a good quantum number. These results suggest that isospin is more strongly broken in the experimental data than in the calculation.

However, this hypothesis is not borne out by estimates of the Coulomb matrix element. Guhr and Weidenmüller [27] obtained a value of $\approx$20 keV in the ^{26}Al experimental data by examining the behavior of Δ_3 for the experimental data. The INC$_B$ calculations give a Coulomb matrix element of $\approx$24 keV, which is consistent with the Guhr and Weidenmüller analysis and certainly does not suggest that there should be less isospin breaking in the calculation. It is also important to note that the Δ_3 statistic, as measured by the parameter μ, shows very similar behavior for the two cases.

It remains a puzzle why the spacing distributions for the shell model and the experiment differ as much as they do when Δ_3 for the shell model and experiment appear to agree. One possible explanation could be that levels in ^{26}Al are missing, or that spins and/or parities have been misassigned in the data set; those effects are known [41] to shift spacing distributions in a fashion similar to what has been observed in ^{26}Al. However, the spin, parity, and isospin assignments in ^{26}Al represent the combined results of many different experiments and extensive analyses (see especially Ref. [24]) and are believed to be of the highest quality. Such an explanation would also appear inconsistent with the nearly one-to-one correspondence between experimental positive-parity states and shell-model states described in Ref. [24] and the fact that very similar spacing distributions are also observed in independent data for ^{30}P (also listed in Table III).

A second explanation could be that for some reason the shell model does not reproduce the short-range correlations. This does not seem likely, because the shell model with isospin conserved produces good agreement with the Wigner distribution. A third possible explanation is that the experimental value of the Coulomb matrix element may be even larger than 24 keV. As discussed above, the isospin mixing in INC$_B$ is determined primarily by the Thomas-Ehrman shift of the $s_{1/2}$ orbit. In this context, the experimental data would suggest that the effective Thomas-Ehrman shift for the $s_{1/2}$ component of the excited states in ^{26}Al is as large or even larger than the 400 keV observed in $A = 17$. However, as we discussed above, a full many-body treatment of this issue is not available at present. The extraction of the Coulomb matrix element for these data by Guhr and Weidenmüller [27] utilized only Δ_3, and a determination of the Coulomb matrix element directly from the spacing distribution has not been performed. We note that there is evidence [41] that Δ_3 values for small sample sizes are much more variable

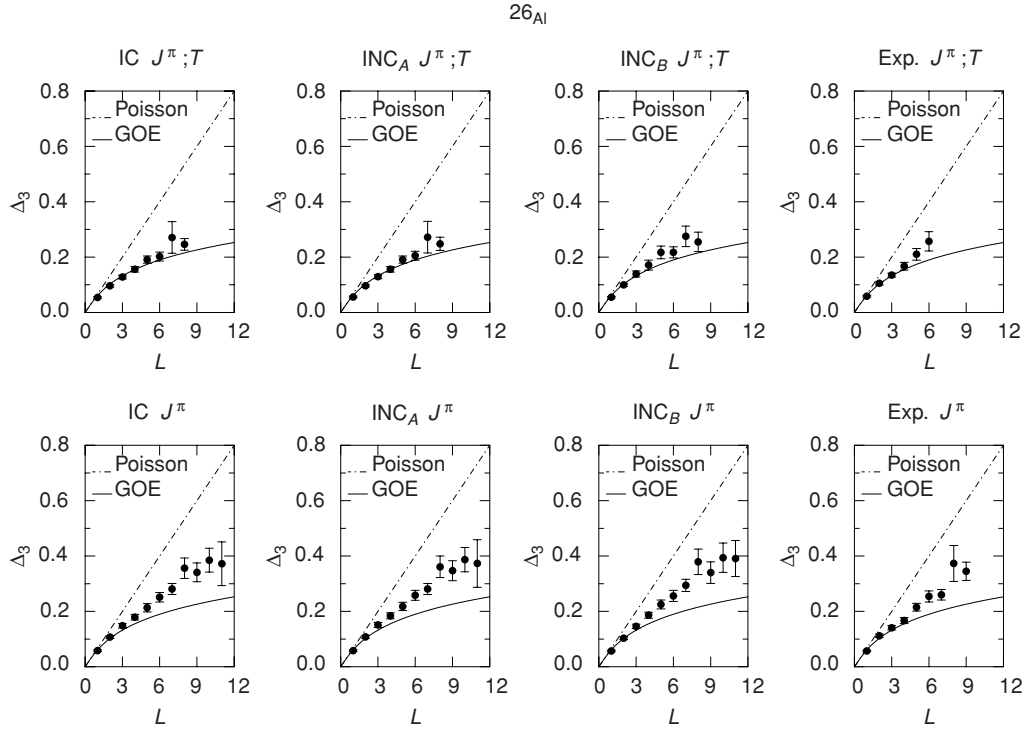

FIG. 3. Δ_3 for shell-model eigenvalues and experimental eigenvalues in ^{26}Al. The labels on each graph indicate which quantum numbers identify the sequences and which Hamiltonian was used in the calculation. Solid curves show GOE distributions, and dashed curves show the corresponding Poisson distributions.

than spacing distributions; this allows the possibility that the spacing distribution might be consistent with a larger matrix element.

V. TRANSITION ANALYSES

The original motivation for this study was the question of how a broken symmetry affected the distribution of reduced transition probabilities. In this section, we begin to address that issue, first by demonstrating that indeed the distributions are affected in some cases and then by examining whether the calculated distributions are consistent with available experimental data.

The distributions for the IC and INC$_B$ calculations in ^{26}Al are illustrated in Fig. 5. Histogram bins have been chosen so that they would have equal probability if the distribution were Porter-Thomas.

The $M1_{\rm IS}$ and $E2_{\rm IV}$ transition sequences are noticeably affected when the isospin is broken, while the $M1_{\rm IV}$ and $E2_{\rm IS}$ transitions appear to change relatively little. A simple explanation for this is that the strongly affected transition sequences are on average much weaker than those that show little effect [the average values of $B(M1)$ and $B(E2)$ are listed in Table II]; therefore, even a small admixture of the larger partner can have a significant effect. Likewise, the larger transition probabilities show smaller changes when isospin is broken because a small admixture of an effect that is already relatively small has little effect. There are several different ways to quantify these effects. One can compare the average $B(M1)$ and $B(E2)$ values for all calculations in Table II: when isospin is broken the average $B(M1)$ value for isoscalar transitions increases by factors of 10–50 over the value when isospin is conserved, while the average $B(E2)$ values for isovector transitions increase by factors of 2–7. On the other hand, the average $B(M1)$ values for isovector transitions and $B(E2)$ values for isoscalar transitions decrease, but by much smaller amounts ranging from 6–14%. One can also utilize the statistical entropy defined in Eq. (11) as a relative quantitative measure. Values of this quantity are listed in Table IV and show that the trends described above for these ^{26}Al calculations are also present in the ^{22}Na and ^{34}Cl calculations.

It is interesting that the $E2_{\rm IS}$ distributions appear to differ from the Porter-Thomas distribution even for the IC calculations. In fact, a Kolmogorov-Smirnov test [47] suggests that each of these four IC distributions differs from the Porter-Thomas distribution with a statistical significance of $>98\%$. Brown and Bertsch [48] have shown that for shell-model basis-vector amplitudes to follow a Gaussian distribution (equivalent to the Porter-Thomas distribution for widths), the level spacing must be comparable to the off-diagonal matrix elements, a condition that is not satisfied at the lower energies of these calculations.

To put these results in perspective, we show experimental results for ^{30}P in Fig. 6; we choose to show ^{30}P data rather than ^{26}Al data because there is insufficient information on the $M1_{\rm IS}$ and $E2_{\rm IV}$ transition sequences in ^{26}Al to perform a statistical analysis.

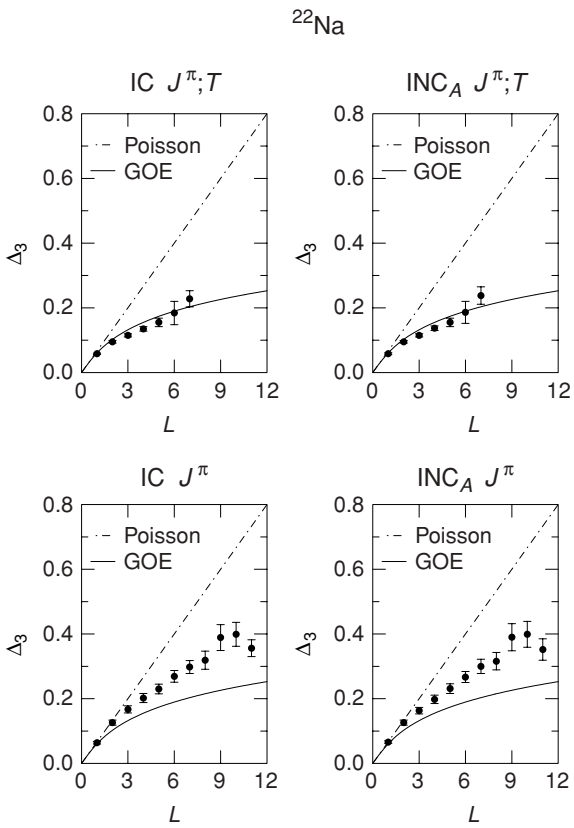

FIG. 4. Δ_3 for shell-model eigenvalues in ^{22}Na. The labels on each graph indicate which quantum numbers identify the sequences and which Hamiltonian was used in the calculation. Solid curves show GOE distributions, and dashed curves show the corresponding Poisson distributions.

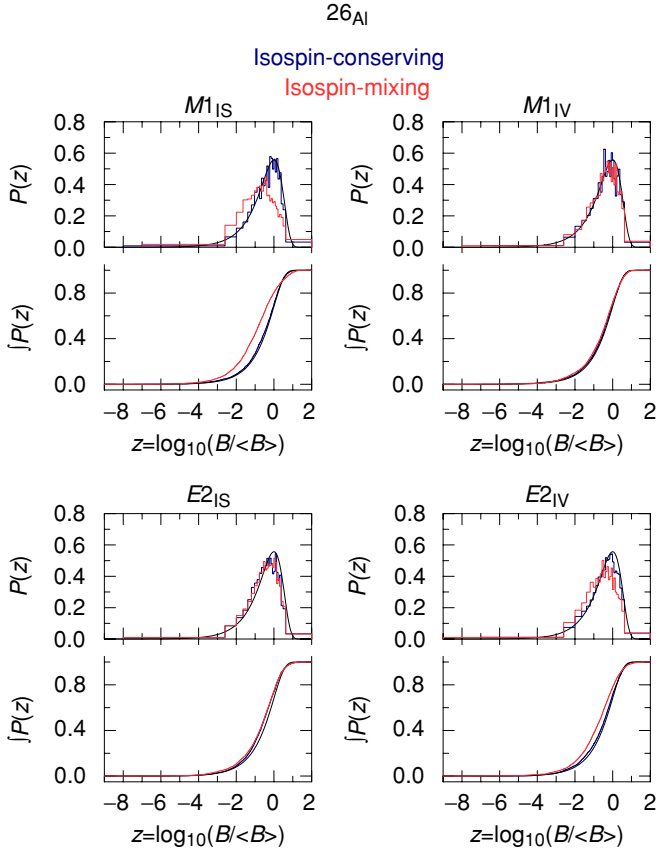

FIG. 5. (Color) distributions of reduced transition probabilities for the IC (in red) and INC$_B$ (in blue) calculations. The smooth black curves show the Porter-Thomas distribution.

Details of the data and its analysis have been given in Ref. [30]. We note that in each of the four $L = 1$ sequences, the experimental distributions lie below the Porter-Thomas distributions at small values of z (in contrast with the shell-model calculations); this is especially noticeable in the cumulative probability plots and is assumed to represent the experimental difficulties in measuring weak transitions. The $E2$ sequences do not show such effects; many of these $B(E2)$ values were obtained from mixed $M1/E2$ transitions, and the combined width allowed the relatively weak part to be determined as well. Both sets of $B(E2)$ distributions show a cumulative probability above the Porter-Thomas distribution, which is consistent with the shell-model calculations, and the $E2_{\mathrm{IV}}$ transitions are farther from the Porter-Thomas, which is also consistent with the calculations.

Combining the different $M1$ and $E2$ experimental transition sequences for ^{26}Al and ^{30}P reduces some of the statistical limitations and provides a different perspective. The combinations are shown in Fig. 7.

As expected, the lack of weak transitions is very evident, but another common feature is the fact that both probability density functions peak at $z \approx -0.4$. While it is true that the missing weak transitions distort the distribution, the observed distributions are not consistent with a Porter-Thomas distorted by missing levels. In fact, they are very similar to the combined distributions for the shell-model calculations with broken isospin, which are shown in Fig. 8.

The probability density function has a maximum at $z \approx -0.5$ for each of the four sets of INC calculations. Therefore, the isospin breaking is very evident in the transition distributions, even for those cases where it had little effect on the eigenvalue distributions. This is an important result because (1) it offers further confirmation that the types of distortion from the Porter-Thomas distribution observed in experimental data are consistent with being a signature of isospin mixing and (2) it emphasizes that different statistics have sharply different sensitivities to a broken symmetry. In this case, the eigenvalues

TABLE IV. Entropy values for different transition sequences. A more negative value indicates greater disagreement with the Porter-Thomas distribution.

Nuclide	Hamiltonian	$M1_{\mathrm{IS}}$	$M1_{\mathrm{IV}}$	$E2_{\mathrm{IS}}$	$E2_{\mathrm{IV}}$
^{22}Na	IC	−0.35	−0.27	−0.36	−0.29
	INC$_A$	−0.57	−0.27	−0.30	−0.33
^{26}Al	IC	−0.32	−0.29	−0.31	−0.33
	INC$_A$	−0.53	−0.33	−0.31	−0.43
	INC$_B$	−0.58	−0.36	−0.33	−0.43
^{34}Cl	IC	−0.30	−0.41	−0.29	−0.29
	INC$_A$	−0.51	−0.33	−0.27	−0.36

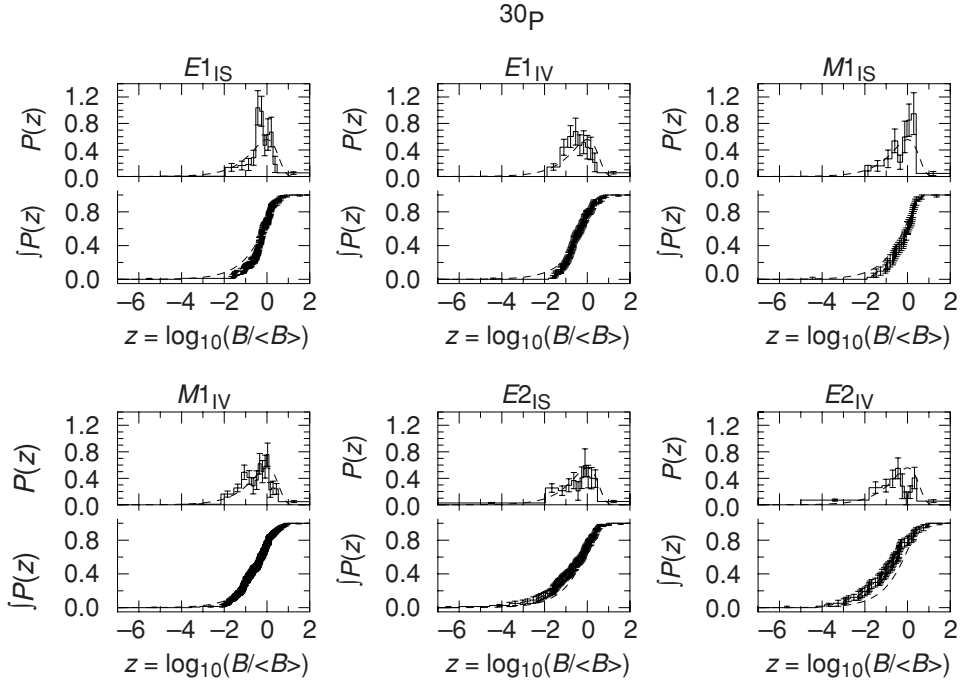

FIG. 6. Distributions of reduced transition probabilities for ^{30}P experimental transition sequences. The dashed curves show the Porter-Thomas distribution.

and eigenvalue statistics for the INC$_A$ calculations show no change from when isospin is conserved, whereas the transition distributions do show a noticeable effect.

Another important aspect of these results is the fact that isospin mixing affects the various transition sequences differently. The effect of symmetry breaking on the eigenvalue distribution is a generic effect that can be explained completely with RMT. The fact that RMT predicts a deviation from the Porter-Thomas distribution is certainly part of the story. However, because the shell model shows that the distributions for different transition sequences are different, then this must be a dynamical effect that cannot be explained completely by

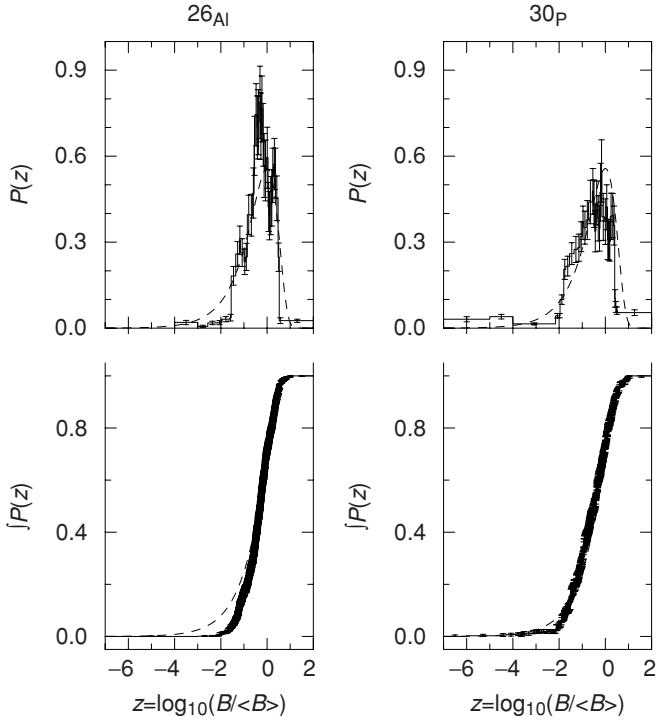

FIG. 7. Combined $M1$ and $E2$ distributions of reduced transition probabilities for ^{26}Al and ^{30}P experimental transition sequences. The dashed curves show the Porter-Thomas distributions.

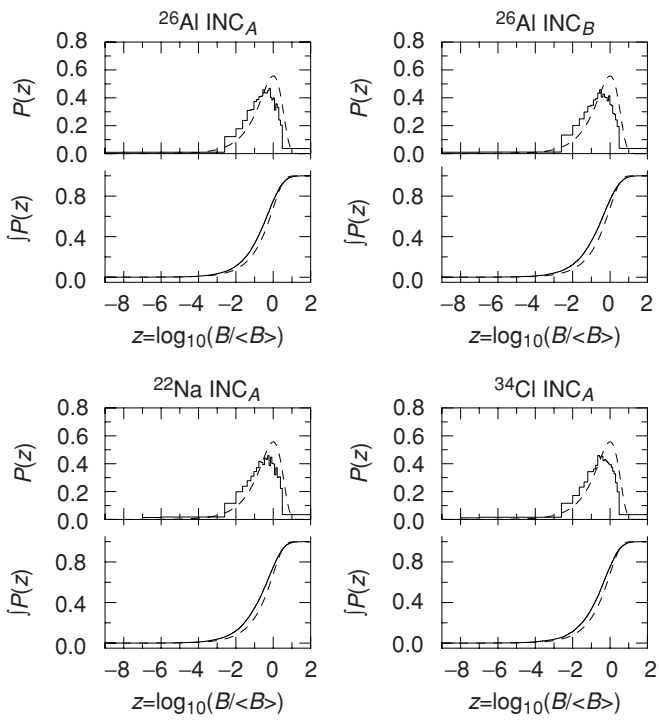

FIG. 8. Combined distributions of reduced transition probabilities for the four shell-model INC calculations. The dashed curves show the Porter-Thomas distributions.

a theory such as RMT. Thus, the approach of using a high statistics "analog" measurement to supplement and confirm the experimental nuclear results is not appropriate, since the results of such a measurement must depend to some degree on the specific dynamics of that system.

VI. CONCLUSION

We have utilized the nuclear shell model to examine how a broken symmetry—in this case isospin—affects both eigenvalue statistics and reduced transition probability distributions. For three nuclides in the *s-d* shell—^{22}Na, ^{26}Al, and ^{34}Cl—calculations have been performed with both conserved isospin and broken isospin; two different isospin-nonconserving calculations were performed for ^{26}Al. The analyses utilized $\approx$100 eigenvalues with spins 0−5 and $B(M1)$ and $B(E2)$ values connecting those states in order to allow comparisons with available experimental data for ^{26}Al and ^{30}P.

For two eigenvalue statistics, the nearest-neighbor spacing distribution and the Δ_3 statistic, the INC calculations utilizing $A = 39$ single-particle energies show little difference from the calculations with isospin conserved. On the other hand, these eigenvalue statistics for INC calculations in ^{26}Al utilizing $A = 17$ single-particle energies do show differences from the IC case. The Coulomb matrix element is approximately four times larger in this second case, and our conclusion is that it is now large enough to affect the eigenvalue statistics. For this particular case, Δ_3 is very similar to that obtained for experimental data, while the NNSD for the shell model still shows some notable differences from the experimental data.

The reduced transition probability distributions also show effects of the broken isospin but in significantly different ways. The effects here depend on which transition sequence is under consideration, as the $M1_{\mathrm{IS}}$ and $E2_{\mathrm{IV}}$ sequences are noticeably affected, whereas the $M1_{\mathrm{IV}}$ and $E2_{\mathrm{IS}}$ sequences are not. The simplest explanation for this is that the transitions that are weaker on average are more strongly affected by the admixtures in the wave functions. The results are qualitatively similar to observations in the experimental data. We find that in contrast to the eigenvalue statistics, both calculations with broken isospin show changes compared to the IC case, although those changes are more significant for the calculation with the larger matrix element.

The fact that transition distributions are affected for all INC calculations emphasizes that the sensitivity of this statistic to the broken symmetry is much higher in this case than that of the eigenvalue statistics. However, that higher sensitivity appears to be due to the dynamics of this particular situation—the relative strengths of isovector and isoscalar transitions—and is not necessarily a general behavior. The fact that transition distributions require information on dynamics and are not generic, as are the eigenvalue statistics, may limit the effectiveness of "analog" experiments to serve as surrogates for other systems and makes very difficult the development of a general theory to describe such distributions.

ACKNOWLEDGMENTS

We thank K. T. Mahar for assistance with the analysis in the early part of this project. One of us (GEM) thanks Y. Alhassid, T. Guhr, and H. A. Weidenmüller for valuable discussions. This work was supported in part by the U.S. Department of Energy, Office of High Energy and Nuclear Physics, under Grant Nos. DE-FG02-96ER40990 and DE-FG02-97ER41042, and by NSF Grant No. PHY-0244453.

[1] E. P. Wigner, in *Statistical Theories of Spectra: Fluctuations*, edited by C. E. Porter (Academic Press, New York, 1965), p. 199.
[2] C. E. Porter and R. G. Thomas, Phys. Rev. **104**, 483 (1956).
[3] T. J. Krieger and C. E. Porter, J. Math. Phys. **4**, 1272 (1963).
[4] F. J. Dyson, J. Math. Phys. **3**, 140 (1962).
[5] F. J. Dyson, J. Math. Phys. **3**, 157 (1962).
[6] F. J. Dyson, J. Math. Phys. **3**, 166 (1962).
[7] F. J. Dyson, J. Math. Phys. **3**, 1191 (1962).
[8] F. J. Dyson and M. L. Mehta, J. Math. Phys. **4**, 701 (1963).
[9] M. L. Mehta and F. J. Dyson, J. Math. Phys. **4**, 713 (1963).
[10] M. L. Mehta, *Random Matrices and the Statistical Theory of Energy Levels* (Academic Press, New York, 1967).
[11] H. I. Liou, H. S. Camarda, S. Wynchank, M. Slagowitz, G. Hacken, F. Rahn, and J. Rainwater, Phys. Rev. C **5**, 974 (1972).
[12] H. I. Liou, H. S. Camarda, and F. Rahn, Phys. Rev. C **5**, 1002 (1972).
[13] W. M. Wilson, E. G. Bilpuch, and G. E. Mitchell, Nucl. Phys. **A245**, 285 (1975).
[14] W. A. Watson, III, E. G. Bilpuch, and G. E. Mitchell, Nucl. Instrum. Methods **188**, 571 (1981).
[15] T. A. Brody, J. Flores, J. B. French, P. A. Mello, A. Pandey, and S. S. M. Wong, Rev. Mod. Phys. **53**, 385 (1981).
[16] O. Bohigas, M. J. Giannoni, and C. Schmit, Phys. Rev. Lett. **52**, 1 (1984).
[17] M. L. Mehta, *Random Matrices* (Academic, New York, 1991), 2nd ed.
[18] N. Rosenzweig and C. E. Porter, Phys. Rev. **120**, 1698 (1960).
[19] T. Guhr, A. Müller-Groeling, and H. Weidenmüller, Phys. Rep. **299**, 189 (1998).
[20] J. F. Shriner, Jr., G. E. Mitchell, and B. A. Brown, Phys. Lett **B586**, 232 (2004).
[21] A. Pandey, Ann. Phys. (NY) **134**, 110 (1981).
[22] P. M. Endt, P. de Wit, and C. Alderliesten, Nucl. Phys. **A459**, 61 (1986).
[23] P. M. Endt, P. de Wit, and C. Alderliesten, Nucl. Phys. **A476**, 333 (1988).
[24] P. M. Endt, P. de Wit, C. Alderliesten, and B. H. Wildenthal, Nucl. Phys. **A487**, 221 (1988).
[25] G. E. Mitchell, E. G. Bilpuch, P. M. Endt, and J. F. Shriner, Jr., Phys. Rev. Lett. **61**, 1473 (1988).
[26] J. F. Shriner, Jr., E. G. Bilpuch, P. M. Endt, and G. E. Mitchell, Z. Phys. A **335**, 393 (1990).

[27] T. Guhr and H. A. Weidenmüller, Ann. Phys. (NY) **199**, 412 (1990).
[28] M. S. Hussein and M. P. Pato, Phys. Rev. C **47**, 2401 (1993).
[29] C. A. Grossmann, M. A. LaBonte, G. E. Mitchell, J. D. Shriner, J. F. Shriner, Jr., G. A. Vavrina, and P. M. Wallace, Phys. Rev. C **62**, 024323 (2000).
[30] J. F. Shriner, Jr., C. A. Grossmann, and G. E. Mitchell, Phys. Rev. C **62**, 054305 (2000).
[31] C. Ellegaard, T. Guhr, K. Lindemann, J. Nygård, and M. Oxborrow, Phys. Rev. Lett. **77**, 4918 (1996).
[32] H. Alt, C. I. Barbosa, H.-D. Gräf, T. Guhr, H. L. Harney, R. Hofferbert, H. Rehfeld, and A. Richter, Phys. Rev. Lett. **81**, 4847 (1998).
[33] A. A. Adams, G. E. Mitchell, and J. F. Shriner, Jr., Phys. Lett. **B422**, 13 (1998).
[34] C. I. Barbosa, T. Guhr, and H. L. Harney, Phys. Rev. E **62**, 1936 (2000).
[35] M. S. Hussein and M. P. Pato, Phys. Rev. Lett. **84**, 3783 (2000).
[36] C. Dembowski, Ph.D. thesis, Technische Universität Darmstadt, 2003.
[37] W. Rae, A. Etchegoyen, and B. A. Brown, OXBASH, the Oxford-Buenos Aires-MSU Shell-Model Code, Technical Report 524, Michigan State University Cyclotron Laboratory, 1985 (unpublished).
[38] W. E. Ormand and B. A. Brown, Nucl. Phys. **A491**, 1 (1989).
[39] T. A. Brody, Lett. Nuovo Cimento **7**, 482 (1973).
[40] T. H. Seligman and J. J. M. Verbaarschot, J. Phys. A **18**, 2227 (1985).
[41] J. F. Shriner, Jr., and G. E. Mitchell, Z. Phys. A **342**, 53 (1992).
[42] W. E. Ormand and R. A. Broglia, Phys. Rev. C **46**, 1710 (1992).
[43] Y. Alhassid and R. D. Levine, Phys. Rev. Lett. **57**, 2879 (1986).
[44] Y. Alhassid and M. Feingold, Phys. Rev. A **39**, 374 (1989).
[45] Y. Alhassid and A. Novoselsky, Phys. Rev. C **45**, 1677 (1992).
[46] D. C. Meredith, Phys. Rev. E **47**, 2405 (1993).
[47] W. H. Press, S. A. Teukolsky, W. T. Vetterling, and B. P. Flattery, *Numerical Recipes in Fortran 77: The Art of Scientific Computing* (Cambridge University Press, New York, 1992), 2nd ed.
[48] B. A. Brown and G. Bertsch, Phys. Lett. **B148**, 5 (1984).